ANTIOXIDANTS & REDOX SIGNALING
Volume 10, Number 9, 2008

DOI: 10.1089/ars.2008.2055

Forum Original Research Communication

The Catalytic Site of Glutathione Peroxidases

Silvio C. E. Tosatto,[1] Valentina Bosello,[2] Federico Fogolari,[3] Pierluigi Mauri,[4] Antonella Roveri,[2] Stefano Toppo,[2] Leopold Flohé,[5] Fulvio Ursini,[2] and Matilde Maiorino[2]

Abstract

In GPxs, the redox-active Se or S, is at hydrogen bonding distance from Gln and Trp residues that contribute to catalysis. From sequence homology of >400 sequences and modeling of the *Dm*GPx as a paradigm, Asn136 emerged as a fourth essential component of the active site. Mutational substitution of Asn136 by His, Ala, or Asp results in a dramatic decline of specific activity. Kinetic analysis indicates that k_{+1}, the rate constant for the oxidation of the enzyme, decreases by two to three orders of magnitude, whereas the reductive steps characterized by k'_{+2} are less affected. Accordingly, MS/MS analysis shows that in Asn136 mutants, the peroxidatic Cys45 stays largely reduced also in the presence of a hydroperoxide, whereas in the wild-type enzyme, it is oxidized, forming a disulfide with the resolving Cys. Computational calculation of pK_a values indicates that the residues facing the catalytic thiol, Asn136, Gln80, and, to a lesser extent Trp135, contribute to the dissociation of the thiol group, Asn136 being most relevant. These data disclose that the catalytic site of GPxs has to be redrawn as a tetrad, including Asn136, and suggest a mechanism accounting for the extraordinary catalytic efficiency of GPxs. *Antioxid. Redox Signal*. 10, 1515–1525.

Introduction

GLUTATHIONE PEROXIDASES (GPxs) catalyze the reduction of hydroperoxides to alcohols and the concomitant oxidation of thiols to disulfides. The glutathione peroxidase family is named after bovine tetrameric GPx-1, the first GPx described (36) and the first mammalian protein in which selenium was identified (19). The first monomeric selenocysteine-containing GPx (PHGPx or GPx-4) (50) was described some years later, followed soon by the Sec-containing tetrameric GPx-3 (43) and GPx-2 (9). Since then, a large number of homologous sequences from organisms of all living kingdoms have been annotated in the data banks, most of them containing a Cys residue corresponding to the Sec present in most of the vertebrate enzymes. It thus became evident that the members of the GPxs family, with a Sec as redox active moiety, are just a minor group, confined to vertebrates, with some scattered presence in lower organisms. Despite structural similarities, not all of the GPx homologues are preferentially reduced by GSH but by thioredoxin (Trx) or related proteins (26, 33, 41, 42). The majority of nonvertebrate GPxs share structural features indicating a preferential reactivity with Trx (33). These Trx peroxidases of the GPx family are monomeric enzymes containing a second, nonaligned, Cys within the α2 helix. On oxidation, the peroxidatic cysteine forms a disulfide bridge with this second cysteine, which, in analogy to the catalytic cycle of peroxiredoxins, acts as a "resolving cysteine" (C_R) in being indispensable for regeneration of the ground-state enzyme *via* reduction by Trx (26, 33, 41, 44).

The biologic role of GPxs had primarily been seen in the detoxification of hydroperoxides. By removing hydroperoxides, the enzymes were thought to prevent homolytic or heterolytic decomposition of hydroperoxides, which would produce reactive radicals, and, indeed, some of the GPxs, in particular the mammalian GPx-1, play a pivotal role in cellular antioxidant defense (17). Over the last two decades, however, evidence accumulated that hydroperoxides are also involved in cell signaling (53), and that reactions carried out by GPxs could participate in signal transduction, ei-

[1]Department of Biology and CRIBI Biotechnology Centre and [2]Department of Biological Chemistry, University of Padova, Padova; [3]Department of Biomedical Sciences, University of Udine, Udine; and [4]Institute for Biomedical Technologies, National Research Council, Milano, Italy.
[5]MOLISA GmbH, Magdeburg, Germany.

ther dampening the oxidative signal or targeting it to specific protein thiols. Thus, apart from counteracting oxidative stress, the physiologic function of GPxs expands to physiologic processes in which lipoxygenase or cyclooxygenase activity or protein thiol oxidation plays a crucial role (7, 51). GPxs have been implicated in modulating inflammation (3, 4, 54), proliferation (55), apoptosis (24), maturation of spermatozoa (32, 48), activation of transcription factors (12), and cytokine-induced gene activation (5).

Structural analyses of enzymes of the GPxs family (14, 26, 27, 39, 44) revealed that they share the $\alpha\beta$ fold of thioredoxin (34). Redox catalysis takes place on a selenocysteine (Sec) or Cys residue (15, 56), located on a flat surface of the protein, N-terminally to the α1 helix. Interestingly, this peroxidatic cysteine residue (C_P) corresponds to the N-terminal Cys residue of the CysXXCys motif of Trx (21, 34). From the three-dimensional structure of the bovine GPx-1, as was established in 1983 (14), a catalytic triad composed of a Sec, a Trp, and a Gln residue was deduced. It was found to be typical of all GPxs and shown to be functionally relevant by mutational analysis of porcine GPx-4 (30) and more recently also in a nonselenium GPx-type tryparedoxin peroxidase from *Trypanosoma brucei* (*Tb*GPxIII) (41). In this triad, the amido and imino groups of the Gln and Trp residues are in hydrogen-bonding distance from the selenium (or sulfur) of the peroxidatic Sec or Cys and have been proposed to activate the redox element (the selenol or the thiol) by hydrogen bonding, which facilitates the nucleophilic attack on the hydroperoxide (30). On collision with a hydroperoxide, the active-site selenium or sulfur is therefore readily oxidized to a selenenic or sulfenic acid derivative, respectively, which thereafter must be reduced to terminate the catalytic cycle. In enzymologic terms, these deductions imply an enzyme-substitution mechanism that, in kinetic terms, should be reflected in a ping-pong pattern, as is indeed observed (42, 49).

Despite the seemingly compelling evidence how GPxs exert their catalysis, the commonly accepted view must be amended. Sequence alignment of GPxs, encompassing to date >400 proteins, and improved structural knowledge highlighted further elements that might contribute to catalysis. From the present study, carried out on the *Drosophila melanogaster* GPx (*Dm*GPx) as a paradigm for the entire GPx family, we provide evidence that it is not a triad, but a tetrad that accounts for the extraordinary catalytic efficiencies of glutathione peroxidases. An asparagine residue, Asn136 in *Dm*GPx, complements Gln80 and Trp135 and proved to be even more important in C_P activation than any of the residues so far implicated.

Materials and Methods

Multiple sequence alignment

The alignment of proteins containing an annotated glutathione peroxidase domain and molecular modeling of *Dm*GPx (Swiss-Prot accession number Q9VZQ8) was collected by running PSI-BLAST (1) for four iterations with default parameters. A multiple-sequence alignment of 422 unique sequences was generated with MUSCLE (13). From these, a subset of seven sequences was manually selected to represent the sequence variability among the different species and was drawn by using Espript (22).

Molecular modeling

The structure of *Dm*GPx was modeled from the crystal structure of the selenocysteine-to-glycine mutant of human GPx-4 (PDB code: 2GS3). The alignment between both sequences is shown as part of Fig. 1. The model, covering the *Dm*GPx sequence (residues 10 to 165) corresponding to the crystallized *Homo sapiens* GPx-4 structure shown in Fig. 1, was constructed from the alignment by using the HOMER server (URL: http://protein.cribi.unipd.it/). The server uses the conserved parts of the structure to generate a raw model, which is then completed by modeling the divergent regions with a fast divide-and-conquer method (46). Side chains are placed with SCWRL3 (8), and the final energy evaluated with FRST (45).

Evolutionary trace analysis

Evolutionary trace, expressed as sequence-conservation patterns, is often used to derive functional constraints on protein evolution (47). Consurf (28) was used to map the sequence conservation onto the model structure with standard parameters, except for the number of PSI-BLAST iterations (four instead of one) and maximum number of homologues (500 instead of 50). Both parameters were increased to allow a better sequence-space coverage. The results were visualized with PyMol (URL: http://pymol.sourceforge.org/).

Preparation, expression and purification of recombinant wild type DmGPx and mutants

The expression vector pQE30 (Qiagen, Hilden, Germany) containing the full-length *Dm*GPx cDNA was obtained as reported (33), and was designed to yield a product containing the N-terminal extension MRGHHHHHHGSAC upstream of position 2 of the authentic sequence. This construct was mutated at residues Asn136, Asn40, and Cys74 to yield the variants N136A, N136H, N136D, N40A, and C74A, respectively by means of the QuikChange site-directed mutagenesis kit (Stratagene, Cedar Creek, TX) by using the primers (changed codons in italics):

fw: 5′-CAGCGGAATCAAGTGG*GCC*TTCACCAAGTTTC-TGGTGAAC-3′
rev: 5′-GTTCACCAGAAACTTGGTGAA*GGC*CCACTTGA-TTCCGCTG-3′
fw: 5′-CAGCGGAATCAAGTGG*CAC*TTCACCAAGTTTC-TGGTGAAC-3′
rev: 5′-GTTCACCAGAAACTTGGTGAA*GTG*CCACTTGA-TTCCGCTG-3′
fw: 5′-CAGCGGAATCAAGTGG*GAC*TTCACCAAGTTTC-TGGTGAAC-3′
rev: 5′-GTTCACCAGAAACTTGGTGAA*GTC*CCACTTGA-TTCCGCTG-3′
fw: 5′-GCAAGGTGGTCCTGGTGGTG*GCC*ATCGCCTCCA-AGTGCGG-3′
rev: 5′-CCGCACTTGGAGGCGAT*GGC*CACCACCAGGA-CCACCTTGC-3′
fw: 5′-GTGATCCTCAACTTCCCG*GCC*AATCAGTTTGGG-TCCCAG-3′
rev: 5′-CTGGGACCCAAACTGATT*GGC*CGGGAAGTTGA-GGATCAC-3′

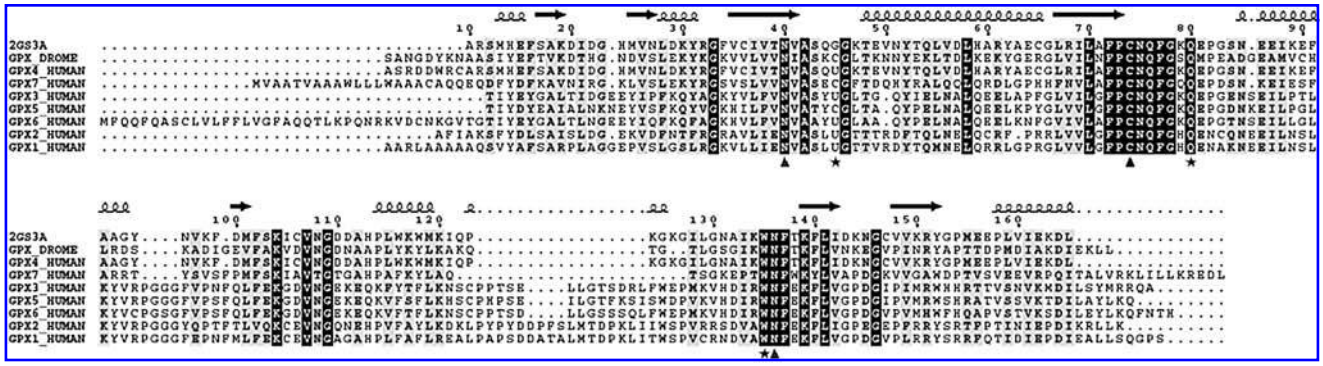

FIG. 1. Multiple-sequence alignment of representative GPx sequences. The sequence of the crystal structure with PDB code 2GS3 is shown in the first row, with the secondary structure above. Sequence numbering follows *Drosophila* GPx, and all seven human GPx sequences are also shown. *Residues composing the established catalytic triad. Δ, The two strictly conserved asparagine and the cysteine residues. Note that the catalytic cysteine is mutated to glycine in the crystal structure (first row).

Mutations were verified by double-strand DNA sequencing.

Protein expression induced in *E. coli* JM 109 by 1 m*M* IPTG for ~4 h. After lysis of the bacterial pellet by B-Per extraction reagent (Pierce, Rockford, IL) containing 5 m*M* mercaptoethanol, 0.1 mg/ml phenylmethylsulfonyl fluoride, 0.7 mg/ml pepsatin, and 0.5 mg/ml leupeptin, protein purification was obtained by two chromatographic steps on a Ni-NTA (Qiagen, Hilden, Germany) and Superdex 75 resins, as previously described (33). After concentration, protein content was quantified according to (6). The purified proteins appeared 80% homogeneous on SDS-PAGE gels stained with Coomassie blue. Before use, the enzymes were reduced by 30 m*M* 2-mercaptoethanol, as previously described (33).

Circular dicroism spectra of wild-type *Dm*GPx and N136A, N136H, N136D, N40A, and C74A mutants were identical, suggesting that mutations did not produce any detectable structural modification of the overall secondary structure and conformation.

Preparation, expression, and purification of recombinant human Trx and Plasmodium falciparum thioredoxin reductase

Human Trx (*h*Trx) and *Plasmodium falciparum* thioredoxin reductase (*Pf*TrxR) were used for activity measurements and kinetic analysis (see later). These were obtained as recombinant proteins after heterologous expression in *E. coli* and purification. Both the pQE30 plasmids containing the full cDNA sequence of *h*Trx and *Pf*TrxR were a kind gift of Katja Becker, University of Giessen, Germany, and contained an MRGH-HHHHHGS extension for protein purification. The *h*Trx sequence was mutated to obtain the substitution of Cys72 into Ser, to prevent dimerization (40), yielding $h\text{Trx}^{\text{Cys72/Ser}}$ by means of the QuikChange site-directed mutagenesis kit (Stratagene, Cedar Creek, TX) by using the primers (changed codons in italics):

fw: 5′-GCTTCAGAGTGTGAAGTCAAA*TCC*ACGCCAAC-ATTCCAG-3′
rev: 5′-CTGGAATGTTGGCGT*GGA*TTTGACTTCCACTCT-GAAGC-3′

The proteins were expressed, extracted and purified as reported earlier for the *Dm*GPx variants, except that only one chromatographic step on the Ni-NTA resin was performed. Protein content was quantified as before. $h\text{Trx}^{\text{Cys72/Ser}}$ was 95% pure on an SDS gel (Coomassie stain) and was stored at –80°C in small aliquots containing 10 mg/ml protein, which were defrosted just before use. By similar criteria, *Pf*TrxR was 80% pure and stored at +4°C. One unit of *Pf*TrxR is defined as the amount of enzyme yielding NADPH-dependent production of 2 μmol of 2-nitro-5-thiobenzoate ($\varepsilon_{412\text{nm}}$ = 13.6 m*M*/cm) per minute at room temperature in the dithionitrobenzoic acid–reduction assay (23, 37).

Activity measurements and kinetic analysis

The coupled assay with NADPH, Trx, and TrxR was used for activity measurements and kinetic analysis (33, 50). In brief, for activity measurement, absorbance at 340 nm was measured with a Beckman DU7 spectrophotometer equipped with magnetic stirrer at room temperature in a 2.5-ml assay containing 0.1 *M* Tris-HCl (pH 7.4), 5 m*M* EDTA, 0.1% Triton X-100 (vol/vol), 0.15 m*M* NADPH, 5 μ*M* $h\text{Trx}^{\text{Cys72/Ser}}$, and 1 unit/ml of *Pf*TrxR. The reaction started with 30 μ*M* phosphatidylcholine hydroperoxide (PCOOH) (31).

Kinetic analysis was performed by single-curve progression analysis in which reactions run to completion. To this end, the digitalized readouts obtained every second by the spectrophotometer were integrated and divided in time intervals of 5–10 s, where the rate was measured, while the actual substrate concentrations were extrapolated at the beginning of each time interval. Data were fitted to the general Dalziel equation for ping-pong mechanism involving two substrates:

$$[E_0]/v = \phi_0 + \phi_1/[\text{ROOH}] + \phi_2/[\text{Trx}]$$

where $[E_0]$ is the total enzyme molarity, v the rate, [ROOH] and [Trx] the concentrations of the hydroperoxide and Trx, respectively, and the ϕ values are the coefficient experimentally obtained from slopes and intercepts of double-reciprocal Dalziel plot (11). The coefficient ϕ_0 proved to be zero for the Trx peroxidase reaction of *Dm*GPx (33), implying lack

of enzyme saturation, as is commonly observed for the GSH peroxidase reaction of SecGPxs (15, 49). The coefficient ϕ_1 is defined as the reciprocal of the rate constant k'_{+1} for the net forward reduction of reduced enzyme with hydroperoxide (Eq. 1) and may be regarded as k_{+1}, because the reaction shown in Eq. 1 should be irreversible. ϕ_2 is the reciprocal k'_{+2} for the stepwise regeneration of the reduced enzyme by Trx [Eqs. 2 and 3; for a more detailed description, see (33)].

$$GPx_{red} + ROOH \underset{k_{-1}}{\overset{k_{+1}}{\rightleftharpoons}} GPx_{ox} + ROH + H_2O \quad \text{(Eq. 1)}$$

$$GPx_{ox} + Trx\text{-}(SH)_2 \underset{k_{-2}}{\overset{k_{+2}}{\rightleftharpoons}} [GPx_{ox} \cdot Trx\text{-}(SH)_2] \quad \text{(Eq. 2)}$$

$$[GPx_{ox} \cdot Trx\text{-}(SH)_2] \underset{k_{-3}}{\overset{k_{+3}}{\rightleftharpoons}} GPx_{red} + Trx\text{-}(S)_2 \quad \text{(Eq. 3)}$$

Under the adopted conditions, spontaneous reduction of PCOOH was close to zero and was ignored.

pK$_a$ calculations

The computation of pK_a shifts was performed according to the procedure described by Antosiewicz *et al*. (2), with minor modifications as described (20). Histidine neutral state was assigned by using pdb2gmx, one of the utilities of the software package GROMACS (52). First electrostatic energies described as background (*i.e.*, interaction between single ionization charges and the system with nonionized residues), self (desolvation) and interaction (*i.e.*, between ionization charges) energies are computed for all titratable sites in both folded protein and isolated amino acids, which are assimilated, as far as pH-dependent behavior is concerned, to the unfolded protein. Based on these computations, the titration energy in the protein is compared with that in the isolated residue. The energy difference results in a shift in pK_a. Because of the interaction of titrating residues in the second stage, the computed energies are used in a Monte Carlo procedure to generate a statistical ensemble of protonation states at different pH values ranging, for the sake of fitting titration curves, from −2.0 to 16.0 (20). Titration curves for each titratable site are fitted to a single-site ionization curve, and the apparent pK_as are obtained.

Mass spectrometry analysis

Wild-type *Dm*GPx and its Asn136 variants (N136A, N136H, N136D) were reduced by 10 m*M* mercaptoethanol. After removal of the reductant by buffer exchange, the enzymes were treated with 50 μM H_2O_2 for 2 min to obtain oxidation. The oxidized proteins were then characterized by LC-ESI-MS/MS as described (35).

Results

Structural denominators common to the family of GPxs

The availability of both a large number of GPx sequences and high-resolution crystallographic data of GPxs (14, 26, 39), in particular those of the human GPx-4 (PDB code 2GS3), substantially expands the bioinformatics basis to deduce functional characteristics that are common to the entire enzyme family (44). It is therefore deemed worth reconsidering the frequently reproduced catalytic triad of the glutathione peroxidases, as it was deduced from the crystallographic analysis of bovine GPx-1 (14), in view of recent data.

A representative subset of GPx sequences is shown in Fig. 1. Apart from the established catalytic triad (marked with an asterisk), the alignment shows some clusters of amino acids that are highly conserved throughout the entire family, *e.g.*, the NVA(S/T) motif two residues N terminal to the peroxidatic residue (U/C) followed by a strictly conserved xxT, the FPC-NQFGx motif preceding the Gln of the triad, a KxxVNG motif, and the WNFxKxLxxxxG comprising the active site Trp. The residues specifically addressed here (*i.e.*, Asn40, Cys74, and Asn136) are marked with a triangle. The functional relevance of the conserved clusters remains largely unknown, but becomes in part conceivable from Fig. 2, which shows the position-specific conservation in a molecular model of *Dm*GPx, calculated with Consurf (28) from an alignment of 422 sequences. The most conserved residues are clearly located inside a cone extending from the active site toward the opposite protein surface. They comprise not only the three previously documented residues of the catalytic triad, but also a group of residues in the core that are hydrophobic, with the notable exception of Asn40, Asn136, and Cys74, the latter reaching the surface opposite to the catalytic center. Whereas Asn40 and Asn136 are conserved in 100% of the sequences, Cys74 is substituted by Ser or Ala in 5% or 4% of the sequences, respectively.

Figure 3 shows the *Dm*GPx model with the amino acids that are presumably involved in the oxidative step of the catalysis represented as ball-and-sticks. The active-site residues are locked into position by a complex network of

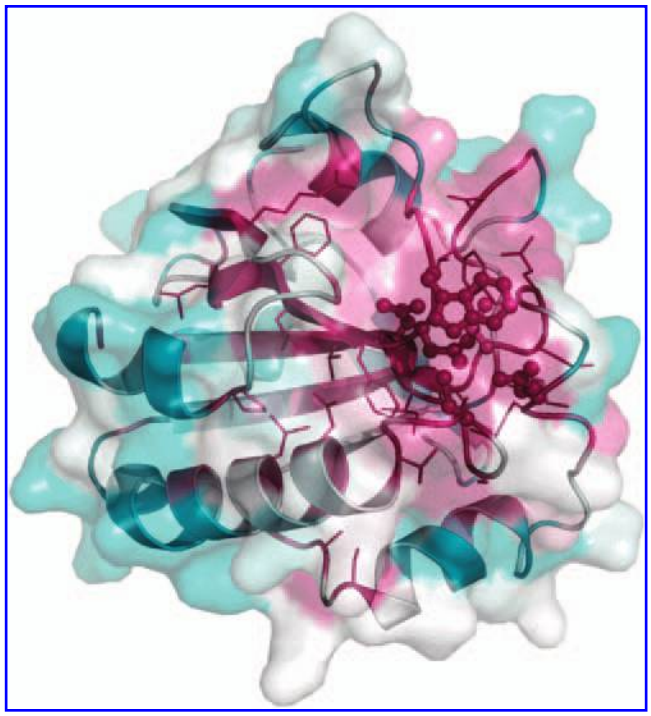

FIG. 2. *Dm*GPx model with Consurf (28) conservation-score coloring from cyan (unconserved) to magenta (strictly conserved). The most-conserved positions are shown as *lines*, and active-site residues in *ball-and-sticks*. The protein surface is semitransparent. (For interpretation of the references to color in this figure legend, the reader is referred to the web version of this article at www.liebertonline.com/ars).

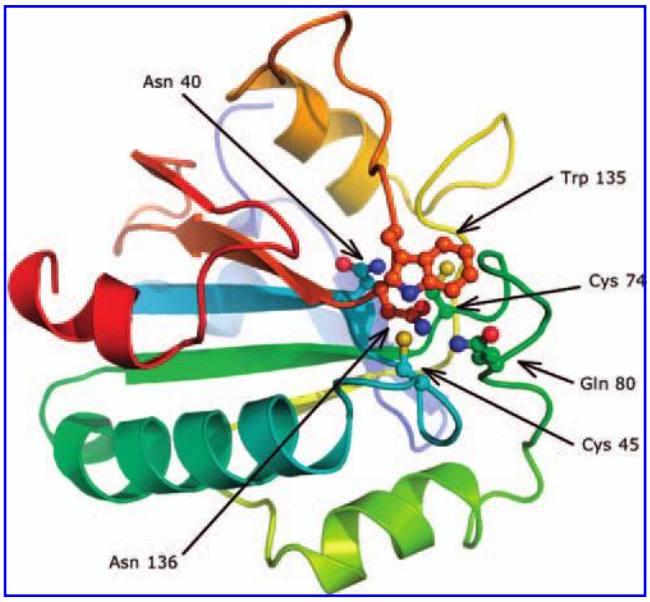

FIG. 3. *Dm*GPx active-site close-up. The protein is shown in the same orientation as in Fig. 2 and colored from N- (blue) to C-terminus (red). Active-site residues discussed in the text are shown as *ball-and-sticks* and labeled. (For interpretation of the references to color in this figure legend, the reader is referrred to the web version of this article at www.liebertonline.com/ars).

hydrogen bonds with neighboring residues (Fig. 4A–C). The Cys45 of *Dm*GPx, which replaces the selenocysteine residue of the mammalian GPxs and is known to be the C_P, forms two strong hydrogen bonds with Thr48 (Fig. 4A), conserved in 95% of the 422 sequences, and corresponds to the second Cys of redox center in most (non-GPx) proteins belonging to the thioredoxin-like fold. Although evidently important for structural stability of the active site, Thr48 appears to be functionally irrelevant, because the exchange of the equivalent Thr50 in *Tb*GPxIII only marginally affected activity (41). The Gln80 residue is held in place by backbone-to-backbone hydrogen bonds with a poorly conserved Lys44 and the highly conserved Gly78, and a hydrogen bond links the amidic nitrogen of Gln80 to sulfur of C_P (Fig. 4B). The loop containing Trp135 and Asn136 is hydrogen-bonded to the Asn40 side chain, and, most important, the imino and amido nitrogens of Trp135 and Asn136 are hydrogen-bonded to the sulfur of C_P (Fig. 4C). A small cavity is seen between Asn136, Asn40, and Cys74 and the core of the protein. It appears too small to harbor a water molecule and is also flanked by conserved hydrophobic side chains. The cavity, however, allows a flexible rearrangement of the three side chains. Asn136, depending on side-chain rotation, can be either coordinated to C_P, as shown in Fig. 4C, or hydrogen-bonded to Asn40 belonging to the conserved rigid core of the protein. This side-chain rearrangement also leads to hydrogen-bond formation between Asn136 and Cys74, suggesting a concerted motion of all three residues. In this conformation, the hydrogen bond between the amide nitrogen of Asn136 and the sulfur of C_P is lost (Fig. 4D).

In short, the model suggests that Asn136 complements Gln80 and Trp135 in activating the sulfur of C_P, whereas in an alternative configuration, Asn136 has no direct contact to C_P, and the catalytic sulfur is hydrogen-bonded only to the nitrogens Gln80 and Trp135, as originally proposed.

Computational calculation of the pK_a of the peroxidatic cysteine

The computational calculation of the pK_a of C_P in the active site of the modelled *Dm*GPx yields a value of 7.2 (Table 1); *i.e.*, approximately one pH unit below the pK_a of free cys-

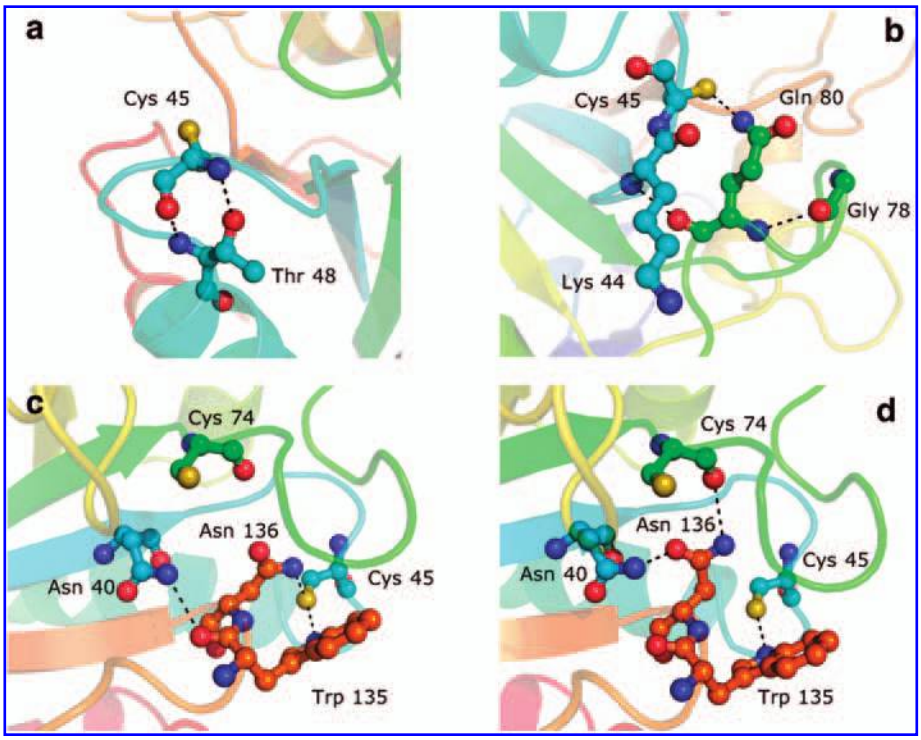

FIG. 4. Hydrogen-bonding network of the *Dm*GPx active site. The protein is shown in different orientations in different panels, colored from N- (blue) to C-terminus (red), to highlight selected details of the active-site geometry. Interaction between (**a**) C_p and T48. (**b**) Q80, K44 and G78. (**c**) N40 and W135. (**d**) N136, N40, and C74. (**b–d**) The hydrogen bonding of sulfur of C_p with nitrogens of W135, N136, and Q80 are also demonstrated. Relevant residues are shown as *ball-and-sticks*, and hydrogen bonds as *black dashes*. See text for explanation. (For interpretation of the references to color in this figure legend, the reader is referred to the web version of this article at www.liebertonline.com/ars).

teine in aqueous solutions, which is low anyway because of proton shuttling between the thiol and the neighboring amino group (16), and two units below the pK_a commonly observed with cysteinyl residues in peptides, *e.g.*, in GSH (25). This corroborates the expected role of the amino acids in the catalytic center of GPx in activating the C_P by favoring its dissociation/activation. To assess the individual roles of Asn136 and the other two residues that are part of the established triad in favoring the activation of C_P, we computed the pK_a values obtained by *in silico* mutation of Asn136, Gln80, and Trp135 in *Dm*GPx (Table 1). The pK_a of C_P was shifted toward more-alkaline values when Ala, Asp, or His replaced the Asn136 residue of the wild-type enzyme. A pK_a shift was also obtained, when Ala, His, or Glu substituted for Gln80. As expected, acidic substitutions produced the largest effect. Surprisingly, a significant effect on pK_a of C_P was obtained only when an acidic residue substituted for Trp135. Accordingly, Asn136 and Gln80 should be the key players in reducing the pK_a of C_P. Notably, the largest pK_a shifts were consistently produced by the exchanges of Asn136, which corroborates a direct interaction of its amido group with the sulfur of C_P, as shown in Fig. 4C.

Effect of mutations of N136 on catalytic activity

Specific activities of molecular mutants of *Dm*GPx proved the presumed role of Asn136 in catalysis. When neutral (Ala) or basic (His) amino acids were substituted for Asn136, the specific thioredoxin peroxidase activity decreased by a factor of 60 or 36, respectively, and the N136D substitution yielded an inactive enzyme (Table 2). The effect on enzymatic activity was also tested on mutants in which the two residues, Asn40 and Cys74, which alternatively could be hydrogen-bonded to Asn136, were mutated into Ala (*Dm*GPx variants N40A and C74A). Mutagenesis of both residues resulted in one third of the specific activity of wild-type enzyme (Table 2).

To determine which step of the catalytic cycle is primarily affected by the substitutions, steady-state kinetic analyses were performed with the wild-type enzyme and the active molecular mutants, and the apparent rate constants for the overall oxidizing and reducing part of the catalytic cycle, k'_{+1} and k'_{+2}, were determined according to Dalziel. As reported (33), *Dm*GPx displays ping-pong kinetics with infinite K_m and V_{max} values. Accordingly, k'_{+1} approximates the rate constant k_{+1}, which describes the oxidation of the enzyme by the hydroperoxide substrate, and k'_{+2} is the net forward-rate constant for the formation of the complex of the oxidized enzyme and the reductant ($k_{+2} - k_{-2}$), here thioredoxin. N136A and N136H substitutions produced a decrease by approximately three orders of magnitude of the apparent rate constant k_{+1}. An influence of the mutations on k'_{+2} also was observed, but was generally less pronounced (Table 3). In agreement with data obtained by specific-activity measurement, a significant, although much less marked, decrease was observed when Ala replaced Asn40 or Cys74.

Table 1. pK_A Values of *Dm*GPxs Peroxidatic Cys

DmGPx Protein	pK_a*
Wild type	7.2
N136A	7.8
N136D	10.2
N136H	7.8
Q80A	7.6
Q80E	9.6
Q80H	7.8
W135A	7.2
W135E	7.6
W135H	7.1

*pK_a values were computed for the wild-type protein or for the indicated Asn136, Gln80, and Trp135 mutants (numeration of *Dm*GPx). Gln80 and Trp135 are part of the established catalytic center of GPxs.

Table 2. Thioredoxin Peroxidase Activity of the Wild Type and Indicated *Dm*GPx Variants

*DmGPx protein**	*Specific activity* (*μmoles/min · mg*)
Wild type	14.38 ± 0.65
N136A	0.24 ± 0.08
N136H	0.40 ± 0.03
N136D	Undetectable
N40A	4.29 ± 0.15
C74A	5.81 ± 0.53

*In the variants, Asn136, Asn40, or Cys74 of the wild-type enzyme was replaced as indicated. Activity was measured with Trx and PCOOH as reducing and oxidizing substrate, respectively, as described in Materials and Methods. Results are means ± SEM of five independent measurements.

Further to confirm the impact of Asn136 on the oxidation of the C_P, the first reaction of the peroxidatic cycle, we analyzed the C_P redox status of wild-type and Asn136 *Dm*GPx variants by MS/MS, after 2-min exposure to 50 μM H_2O_2 in the absence of reducing substrates. In this experiment, the proteins were first reduced, exposed to the oxidant substrate, fragmented, and peptides finally analyzed by MS/MS, as was extensively described for the analysis of wild-type DmGPx (33). A validated procedure was adopted (35), in which peptides were produced by pepsin hydrolysis under acidic conditions to prevent scrambling of disulfides and artifactual cysteine oxidation. The C_P-containing peptides were identified in the three forms: reduced, linked through a disulfide to the fragment containing the C_R, and overoxidized (*i.e.*, with C_P oxidized to a sulfinic acid). As expected, after oxidation by H_2O_2, the wild-type enzyme contained the largest part of the C_P as disulfide with C_R (81%), just traces in the reduced form (2%), and a minor part overoxidized to the sulfinic acid derivative (17%) (Table 4). In contrast, all mutants contained a substantial amount of reduced C_P (36% to 66% for different substitutions), lower amounts of the disulfide, and just traces of the overoxidized form. In agreement with the predictions of molecular modeling and the kinetic data, these results reveal that substitutions at Asn136 yield an enzyme that is more resistant to oxidation.

Discussion

The catalytic triad, in which a Gln and a Trp residue are close to the Sec in the active site of GPx-1, was originally pro-

Table 3. Kinetic Coefficients and Apparent Rate Constants of Wild-Type *Dm*GPx and Molecular Mutants

	Φ_1	k_{+1}	Φ_2	k'_{+2}
DmGPx Protein	(μM s)	($M^{-1}s^{-1}$)	(μM s)	($M^{-1}s^{-1}$)
Wild type*	0.75 ± 0.4	1.3×10^6	0.66 ± 0.2	1.5×10^6
N136A	251 ± 78	4.0×10^3	47 ± 55	2.1×10^4
N136H	176 ± 72	5.7×10^3	27 ± 35	3.7×10^4
N40A	3.7 ± 0.4	2.7×10^5	2.3 ± 1.3	4.3×10^5
C74A	2.4 ± 0.3	4.2×10^5	2.1 ± 0.4	4.6×10^5

Results are means ± SEM of at least three independent measurements. *Values from 33.

posed from crystallographic data (PDB code 1gp1) (14), supported by sequence conservation, and later verified by mutational analysis of GPx-4 (30) and *Tb*GPxIII (41). Thereafter, sequence homology and fold recognition, by using GPx-1 as template, sustained the conclusion that this active site is conserved in all GPxs, including those containing Cys at the active site. In some plant GPx homologues, however, the Gln is replaced by Glu (26), shedding doubt on the absolute requirement of the Gln for catalysis. Conversely, these plant GPxs may be expected to be poor peroxidases, based on data on mutants of the homologous pig GPx4 (30).

In addition, recent higher-definition crystallographic data suggested a reconsideration or amendment of the seemingly convincing concept of the catalytic mechanism. The structure of human GPx-4 (*Hs*GPx-4), which has recently been deposited in structure databases (PDB code 2gs3), confirmed the overall structure of the active site. It differed, however, from the GPx-1 structure (PDB code 1gp1) (14) in a subtle but functionally relevant detail, the orientation of the carboxamide group of Asn136 in the active site. The 1gp1, which is the structure of an over-oxidized enzyme (seleninic form), places the oxygen atom of Asn136 close to the sulfur of C_P. Instead, the structure 2gs3, which represents a mutant with the catalytic Sec replaced by Ala, shows the amide nitrogen of Asn136 pointing toward a position corresponding to the selenium in the wild-type enzyme. Because none of the structures represents the ground-state enzyme, the precise orientation of the Asn remains ambiguous. However, the marked functional consequences of an Asn136 mutation in *Dm*GPx that we observed strongly corroborate the orientation shown in 2gs3, which assumes that in the ground-state enzyme, the amide nitrogen of Asn136 also is hydrogen-bonded to the catalytic sulfur. Only in this position can the Asn activate C_P, because a carbonyl oxygen would hardly support the reactivity of the sulfur. Analogous considerations suggest that the amide nitrogen of Gln80 also is oriented toward the catalytic sulfur. An activation of the C_P sulfur thus appears to be facilitated by hydrogen bonding of the nitrogens of Trp135, Gln80, and Asn136.

Table 4. Redox Status of the Peroxidatic Cys of the Wild Type and *Dm*GPx N136 Variants

DmGPx protein	*Thiol*	*Disulfide*	*Sulfinic*
Wild type	2 ± 0.4*	81 ± 16	17 ± 3
N136A	56 ± 14	41 ± 10	3 ± 1
N136H	36 ± 16	61 ± 20	3 ± 1
N136D	66 ± 17	28 ± 7	6 ± 2

*Results are expressed as means ± SEM of relative percentage of the thiol, disulfide, or sulfinic acid derivatives of the C_P, as determined by MS/MS analysis in three independent experiments after 2 min incubation with 50 μM H_2O_2.

Accordingly, the pK_a shifts between mutant and wild-type GPxs shown in Table 1 were calculated for the configuration in which both amide groups are oriented toward the catalytic thiol. For the Asn configuration chosen, the computed pK_a value of the wild-type *Dm*GPx C_P is 7.2 and thus meets the main demand for the reaction of C_P with hydroperoxides. This decreased pK_a results primarily from a low-barrier hydrogen bond (LBHB) in which the proton is delocalized between the C_P thiol and the amide nitrogen of Asn136. Any alternative orientation of either or both the amide groups would be incompatible with the observed reactivity of C_P. Thiol pK_as of 8.5 and 9.2 are calculated if one or both amide groups are flipped.

However, one must consider that continuum pK_a calculations are not expected to be accurate in absolute terms. Accordingly, the pK values here calculated differ from those recently deduced from pH-dependent rates for cysteine alkylation of the yeast GPx homologue Orp1 by Ma *et al*. (29). Continuum pK_a calculations will, however, reliably predict pK shifts due to changes of the microenvironment of a dissociable residue and, expectedly, Ma *et al*. (29) observed a shift of the deduced pKa of C_P in Orp1 when its active-site Trp and Gln was mutated to Ala. Because the rate of S-alkylation within a protein may not only be modulated by the pKa of the thiol under consideration, it is hard to predict whether the approach chosen by Ma *et al*. (29) or the theoretic one chosen here yields the more revealing data.

Starting from the conformation with both amide groups oriented toward C_P, the largest shifts of the C_P pK_a values are calculated for negatively charged residues substituting for Asn136 and Gln80, whereas substitution by neutral or basic residues yield smaller effects. Qualitatively, the calculated pK_a values are negatively correlated with the activities of molecular mutants of *Dm*GPx, *Tb*GPxIII (41), and the Cys variant of pig GPx-4 (30). The correlation is even better between the pK_a values and the rate constants for the oxidative part of the catalytic cycle, k_{+1}, revealing that the activation of C_P is primarily relevant to the reaction with the hydroperoxide substrate. The particular contribution of Asn136 to the activation/dissociation of C_P, which had so

far been overlooked, is convincingly demonstrated by the complete inactivity of *Dm*GPx N136D and its almost complete resistance to 50 μM H_2O_2 over 2 min, a time frame far beyond that required to oxidize the wild-type enzyme.

Quantitatively, however, the computed pK_a shifts do not fully explain the differing activities of the *Dm*GPx mutants. A pK_a shift of three units, as is calculated for an Asn136/Asp exchange, might well account for the undetectable activity of the mutant and thus may be considered consistent with the assumption that dissociation of C_P is the only pivotal factor for its reactivity, but the rather moderate pK_a elevations calculated for *Dm*GPx N136A or N136H (7.8) do not explain the decrease in k_{+1} values by three orders of magnitude without additional assumptions.

The Trp135 mutations, instead, seem to affect the pK_a values of C_P only marginally, and, in general, corresponding mutations of the pig GPx-4 (30) and the *T. brucei* GPx homologue (41) are apparently less detrimental to enzymatic activity than are corresponding mutations on Gln80 or Asn136. It therefore appears conceivable, as previously proposed (41), that Trp135 is not directly involved in the catalysis, and its primary role is to keep the active-site sulphur or selenium in place by hydrogen bonding. The conservation of the residues Thr48 and Lys44 is likely attributed to a similar strengthening of the active-site architecture (Fig. 4).

The dramatic decrease in activity observed on mutation of Asn136 (Table 2) or Gln80 (30, 41) suggests functional roles of carboxamide groups in GPx catalysis beyond merely enforcing dissociation of C_P. A carboxamide group may also be implicated, in principle, in polarization of the hydroperoxide substrate to facilitate its heterolytic cleavage. For sterical reasons, a direct interaction of Asn136 with substrate can be excluded. Its carboxamide function reaches the redox-active thiol (selenol) from the hydrophobic core of the protein and thus is the ideal candidate to activate C_P. In contrast, the surface-exposed carboxamide of Gln80 can readily interact with both C_P and the substrate. With these considerations, a tentative scheme for the first step of GPx catalysis may be proposed that complies with the vast majority of known sequences, available structures, and mutagenesis data (Fig. 5).

Starting from the thiol form with Trp135, Gln80, and Asn136 coordinated to the sulfur (Fig. 5A), Asn136, due to the low dielectric constant of its hydrophobic environment, most avidly attracts the proton from the C_P thiol to form an LBHB. Because release of the proton from the thiol is further facilitated by the proton-donating power of Trp135 and Gln80, the LBHB between Cys45 and Asn136 is practically equivalent to a salt bridge between the thiolate and the protonated carboxamide group. Panel A in Fig. 5 thus represents the "thiolate" form of the enzyme that can react with the oxidizing substrate. The latter has few structural requirements besides bearing a hydroperoxy group that has access to the surface-exposed sulfur and is likely "bound" in a way that its O-O bond can be polarized by Gln80, as shown in Fig. 5B. In this transition state, the relatively negative carbonyl of Gln80 attracts the proton of the terminal oxygen, whereas its amide donates a proton to the proximal oxygen of the hydroperoxide, thereby generating ROH (instead of RO^-) as a strong leaving group. At the same time, the nucleophilic sulphur can attack the electron-deprived terminal oxygen. On release of the product ROH (or H_2O, if the substrate was H_2O_2; Fig. 5C), we see the sulfenic acid form being generated, which is commonly postulated as the first catalytic intermediate of the catalytic cycle and has recently been verified as such for the GPx-3 protein of *Saccaromyces cerevisiae* (29). In panel C, the sulfenic acid is shown in its S(H)=O tautomeric form, still hydrogen bonded to Asn136. However, the acidic hydrogen will readily dissociate [pK_a values of sulfenic acids are reported to range around 5 (10)], and Gln80 may further reduce the pK_a of the oxidized C_P, as indicated in Fig. 5D. More important, on oxidation and dissociation of the oxidized C_P, the original net of hydrogen bridges at the active site is deeply altered, the carboxamides will shuttle their protons back to conventional tautomeric forms, and the oxidized C_P is largely freed from structural constrains and can reach out to interact with C_R (in case of the thioredoxin-type peroxidases) or the reducing substrate. Asn136 may now adopt its alternative position and become hydrogen-bonded to Asn40 and Cys74, whereby the obligatory movements of C_P for cosubstrate interactions might be further facilitated. This alternate movement of the loop containing Asn136 could account for the minor but significant effect on activity brought about by neutral mutations of Asn40 and Cys74.

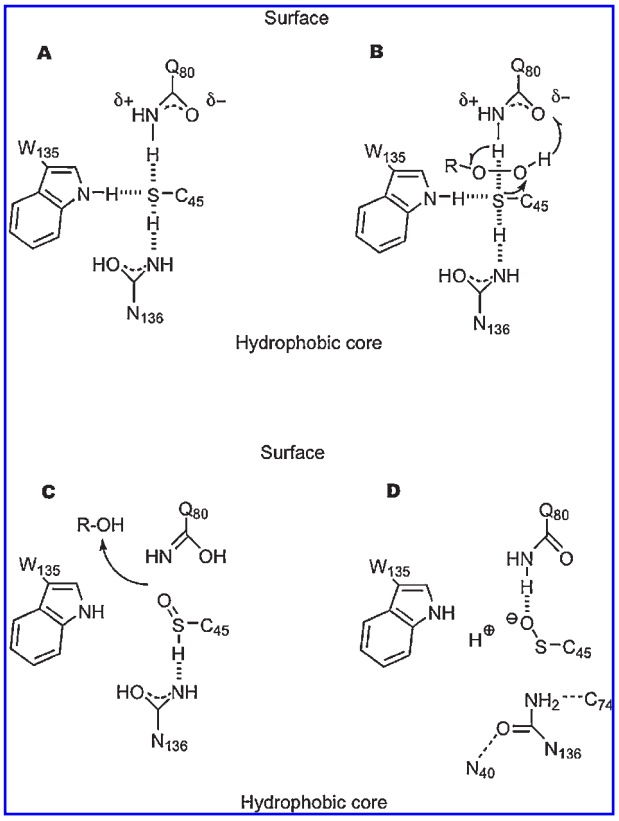

FIG. 5. Proposed scheme for the first step of GPx catalysis.

Figure 5 offers a plausible explanation for reactivity of the C_P of glutathione peroxidases. Extremely high k_{+1} values, which describe the oxidation of the enzymes by hydroperoxide substrates, were not surprising when C_P was Sec, because of the intrinsic higher reactivity of Se *vs*. S. The subsequent discovery of natural, highly reactive Cys-containing GPx homologues was therefore rather unexpected. For instance, the natural cysteine homologue *Dm*GPx, with

a k_{+1} of 1.3×10^6 M/s for the reduction of phosphatidylcholine hydroperoxide, almost reaches the efficiency of the selenoperoxidases. As demonstrated here, this unusual cysteine reactivity is achieved within a catalytic tetrad primarily by two coordinated carboxamide groups, the one of Asn136 being most relevant for C_P activation, whereas that of Gln80, for polarization of the hydroperoxy bond. Figure 5 also reveals how the enzyme is prepared for the next step of the catalytic cycle, the formation of an internal disulfide bridge between C_P and C_R, which is particularly important for the thioredoxin peroxidases of the GPx family. As shown for *Dm*GPx (33) and *Tb*GPxIII (41), this step is obligatory for the consecutive reduction by thioredoxin. As was postulated from molecular modeling (33) and is now evident from the first x-ray structure of a GPx-type thioredoxin peroxidase (26), the formation of this internal disulfide bond requires substantial structural changes, including unwinding of the α2 helix, where C_R (Cys91) is located, plus a major move of C_P, which depends on the disruption of the hydrogen bonds that fix C_P in the catalytic tetrad of the ground-state enzyme. Interestingly, this complicated phenomenon appears not to be the rate-limiting step of the catalysis, because *Dm*GPx kinetics, like those of most GPxs (17), are characterized by a lack of limiting V_{max} and K_m values. This implies that only substrate-involving reactions of the cycle can be rate limiting. In consequence, we cannot conclude how this structural rearrangement is affected by the components of the tetrad, because the step cannot be kinetically analyzed. In contrast, we may argue that the reduction of the disulfide form with thioredoxin is influenced by Asn136, because its substitution also affects k'_{+2} (Table 3). k'_{+2} is best interpreted as the net forward rate constant for the association of the oxidized enzyme, more precisely its disulfide form, with the reducing substrate, here thioredoxin. It is conceivable that Asn-dependent proton shuttling, as is pivotal for the first catalytic step, is also involved in the reductive part of the cycle.

In conclusion, the peroxidatic reaction center of GPx is not a triad, but a tetrad, in which a redox-active cysteine or selenocysteine is hydrogen-bonded to the nitrogens of conserved Asn, Gln, and Trp residues. Within this architecture, the thiol or selenol of C_P is activated, in particular because of the coordination of two carboxamide functions. Beyond the dissociation state of C_P, carboxamide-mediated proton shuttling to polarize further the redox-active chalcogen and the peroxo bond of the substrate must be taken into consideration. In broader perspective, the data presented here disclose a novel structural feature to activate protein thiols (selenols) for the oxidation by hydroperoxides, a phenomenon that merits increasing attention in the context of redox regulation of metabolic processes. Commonly, surface exposure and a nearby positive charge are considered to account for a fast and selective oxidation of particular cysteine residues, and cysteine activation by the positive charge of a coordinated arginine residue is a valid principle, as amply established in peroxiredoxin catalysis (18, 38). It is here demonstrated that rather extreme reaction rates of cysteine residues can also be induced by carboxamide functions of neutral amino acids, if appropriately coordinated, and it might be revealing to search for analogous structural features in proteins with so-far unexplained cysteine reactivities.

Acknowledgments

S.C.E.T. is funded by a "Rientro dei cervelli" grant from the Italian Ministry for Education, University and Research (MIUR). We are indebted to Dr. Louise Benazzi, CNR Milano, for tandem MS analysis.

Abbreviations

C_P, peroxidatic cysteine; C_R, resolving cysteine; *Dm*GPx *Drosophila melanogaster* glutathione peroxidase; GPx, glutathione peroxidase; GPx-1, mammalian glutathione peroxidase-1 (E.C. 1.11.1.9); *h*Trx, human thioredoxin; GPx-4, mammalian glutathione peroxidase-4 (also called PHGPx, E.C. 1.11.1.12); LBHB, low-barrier hydrogen bond; PCOOH, phosphatidylcholine hydroperoxide; PHGPx, phospholipid hydroperoxide glutathione peroxidase (also called GPx-4, E.C. 1.11.1.12); Sec, selenocysteine; *Tb*GPxIII, *Trypanosoma brucei* glutathione peroxidase III; Trx, thioredoxin; *Pf*TrxR, *Plasmodium falciparum* thioredoxin reductase.

References

1. Altschul SF, Madden TL, Schaffer AA, Zhang J, Zhang Z, W. M, and Lipman DJ. Gapped BLAST and PSI-BLAST: a new generation of protein database search programs. *Nucleic Acids Res* 25: 3389–3402, 1997.
2. Antosiewicz J, McCammon JA, and Gilson MK. Prediction of pH-dependent properties of proteins. *J Mol Biol* 238: 415–436, 1994.
3. Banning A and Brigelius-Flohé R. NF-kappaB, Nrf2, and HO-1 interplay in redox-regulated VCAM-1 expression. *Antioxid Redox Signal* 7: 889–899, 2005.
4. Banning A, Deubel S, Kluth D, Zhou Z, and Brigelius-Flohé R. The GI-GPx gene is a target for Nrf2. *Mol Cell Biol* 25: 4914–4923, 2005.
5. Banning A, Schnurr K, Böl GF, Kupper D, Müller-Schmehl K, Viita H, Yla-Herttuala S, and Brigelius-Flohé R. Inhibition of basal and interleukin-1-induced VCAM-1 expression by phospholipid hydroperoxide glutathione peroxidase and 15-lipoxygenase in rabbit aortic smooth muscle cells. *Free Radic Biol Med* 36: 135–144, 2004.
6. Bensadoun A and Weinstein D. Assay of proteins in the presence of interfering materials. *Anal Biochem* 70: 241–250, 1976.
7. Brigelius-Flohé R. Tissue-specific functions of individual glutathione peroxidases. *Free Radic Biol Med* 27: 951–965, 1999.
8. Canutescu AA, Shelenkov AA, and Dunbrack RL. A graph-theory algorithm for rapid protein side-chain prediction. *Protein Sci* 12: 2001–2014, 2003.
9. Chu FF, Doroshow JH, and Esworthy RS. Expression, characterization, and tissue distribution of a new cellular selenium-dependent glutathione peroxidase, GSHPx-GI. *J Biol Chem* 268: 2571–2576, 1993.
10. Claiborne A, Miller H, Parsonage D, and Ross RP. Protein-sulfenic acid stabilization and function in enzyme catalysis and gene regulation. *FASEB J* 7: 1483–1490, 1993.
11. Dalziel K. Initial steady state velocities in the evaluation of enzyme- substrate reaction mechanisms. *Acta Chem Scand*. 11: 1706–1723, 1957.
12. Delaunay A, Pflieger D, Barrault MB, Vinh J, and Toledano MB. A thiol peroxidase is an H2O2 receptor and redox-transducer in gene activation. *Cell* 111: 471–481, 2002.
13. Edgar RC. MUSCLE: multiple sequence alignment with high accuracy and high throughput. *Nucleic Acids Res* 32: 1792–1797, 2004.

14. Epp O, Ladenstein R, and Wendel A. The refined structure of the selenoenzyme glutathione peroxidase at 0.2-nm resolution. *Eur J Biochem* 133: 51–69, 1983.
15. Flohé L. The selenoprotein glutathione peroxidase. In: Dolphin D, Poulson D, Avramovic O, eds. Glutathione: chemical, biochemical, and medical aspects–part A, New York: John Wiley & Sons, 1989.
16. Flohé L, Breitmaier E, Günzler WA, Voelter W, and Jung G. Dissociation behavior of cysteine and related SH-compounds: a 13 C-NMR spectroscopic study on pH dependence of charge distribution. *Hoppe Seylers Z Physiol Chem* 353: 1159–1170, 1972.
17. Flohé L and Brigelius-Flohé R. Selenoproteins of the glutathione system. In: Hatfield D, ed. *Selenium*: *its molecular biology and role in human health*. London: Kluwer Academic Publishers, 2001:157–178.
18. Flohé L, Budde H, Bruns K, Castro H, Clos J, Hofmann B, Kansal-Kalavar S, Krumme D, Menge U, Plank-Schumacher K, Sztajer H, Wissing J, Wylegalla C, and Hecht HJ. Tryparedoxin peroxidase of Leishmania donovani: molecular cloning, heterologous expression, specificity, and catalytic mechanism. *Arch Biochem Biophys* 397: 324–335, 2002.
19. Flohé L, Günzler WA, and Schock HH. Glutathione peroxidase: a selenoenzyme. *FEBS LETT* 32: 132–134, 1973.
20. Fogolari F, Brigo A, and Molinari H. Protocol for MM/PBSA molecular dynamics simulations of proteins. *Biophys J* 85: 159–166, 2003.
21. Fomenko DE, Xing W, Adair BM, Thomas DJ, and Gladyshev VN. High-throughput identification of catalytic redox-active cysteine residues. *Science* 315: 387–389, 2007.
22. Gouet P, Courcelle E, Stuart DI, and Metoz F. ESPript: analysis of multiple sequence alignments in PostScript. *Bioinformatics* 15: 305–308, 1999.
23. Holmgren A and Björnstedt M. Thioredoxin and thioredoxin reductase. *Methods Enzymol* 252: 199–208, 1995.
24. Imai H and Nakagawa Y. Biological significance of phospholipid hydroperoxide glutathione peroxidase (PHGPx, GPx4) in mammalian cells. *Free Radic Biol Med* 34: 145–169, 2003.
25. Jung G, Breitmaier E, Günzler WA, Ottnad M, Voelter W, and Flohé L. 13C NMR studies on the dissociation equilibria of amino thiol compounds. In: Flohe L, Benohr HC, Sies H, et al. eds. *Glutathione*. Stuttgart: Georg Thieme Publishers, 1974:1–15.
26. Koh CS, Didierjean C, Navrot N, Panjikar S, Mulliert G, Rouhier N, Jacquot JP, Aubry A, Shawkataly O, and Corbier C. Crystal structures of a poplar thioredoxin peroxidase that exhibits the structure of glutathione peroxidases: insights into redox-driven conformational changes. *J Mol Biol* 370: 512–529, 2007.
27. Ladenstein R, Epp O, Bartels K, Jones A, Huber R, and Wendel A. Structure analysis and molecular model of the selenoenzyme glutathione peroxidase at 2.8 Å resolution. *J Mol Biol* 134: 199–218, 1979.
28. Landau M, Mayrose I, Rosenberg Y, Glaser F, Martz E, Pupko T, and Ben-Tal N. ConSurf 2005: the projection of evolutionary conservation scores of residues on protein structures. *Nucleic Acids Res* 33: W299–W302, 2005.
29. Ma LH, Takanishi CL, and Wood MJ. Molecular mechanism of oxidative stress perception by the orp1 protein. *J Biol Chem* 282: 31429–31436, 2007.
30. Maiorino M, Aumann KD, Brigelius-Flohé R, Doria D, van den Heuvel J, McCarthy J, Roveri A, Ursini F, and Flohé L. Probing the presumed catalytic triad of selenium-containing peroxidases by mutational analysis of phospholipid hydroperoxide glutathione peroxidase (PHGPx). *Biol Chem Hoppe Seyler* 376: 651–660, 1995.
31. Maiorino M, Gregolin C, and Ursini F. Phospholipid hydroperoxide glutathione peroxidase. *Methods Enzymol* 186: 448–457, 1990.
32. Maiorino M, Roveri A, Benazzi L, Bosello V, Mauri P, Toppo S, Tosatto SC, and Ursini F. Functional interaction of phospholipid hydroperoxide glutathione peroxidase with sperm mitochondrion-associated cysteine-rich protein discloses the adjacent cysteine motif as a new substrate of the selenoperoxidase. *J Biol Chem* 280: 38395–38402, 2005.
33. Maiorino M, Ursini F, Bosello V, Toppo S, Tosatto SC, Mauri P, Becker K, Roveri A, Bulato C, Benazzi L, De Palma A, and Flohé L. The thioredoxin specificity of Drosophila GPx: a paradigm for a peroxiredoxin-like mechanism of many glutathione peroxidases. *J Mol Biol* 365: 1033–1046, 2007.
34. Martin JL. Thioredoxin: a fold for all reasons. *Structure* 3: 245–250, 1995.
35. Mauri P, Benazzi L, Flohé L, Maiorino M, Pietta PG, Pilawa S, Roveri A, and Ursini F. Versatility of selenium catalysis in PHGPx unraveled by LC/ESI-MS/MS. *Biol Chem Hoppe Seyler* 384: 575–588, 2003.
36. Mills GC. Hemoglobin catabolism, I: glutathione peroxidase, an erythrocyte enzyme which protects hemoglobin from oxidative breakdown. *J Biol Chem* 229: 189–197, 1957.
37. Müller S, Gilberger TW, Farber PM, Becker K, Schirmer RH, and Walter RD. Recombinant putative glutathione reductase of Plasmodium falciparum exhibits thioredoxin reductase activity. *Mol Biochem Parasitol* 80: 215–219, 1996.
38. Poole LB. The catalytic mechanism of peroxiredoxins. In: Flohe L, Harris JR, eds. Peroxiredoxin systems, subcellular biochemistry vol 44. New York: Springer, 2007:61–81.
39. Ren B, Huang W, Akesson B, and Ladenstein R. The crystal structure of seleno-glutathione peroxidase from human plasma at 2.9 Å resolution. *J Mol Biol* 268: 869–885, 1997.
40. Ren X, Björnstedt M, Shen B, Ericson ML, and Holmgren A. Mutagenesis of structural half-cystine residues in human thioredoxin and effects on the regulation of activity by selenodiglutathione. *Biochemistry* 32: 9701–9708, 1993.
41. Schlecker T, Comini MA, Melchers J, Ruppert T, and Krauth-Siegel RL. Catalytic mechanism of the glutathione peroxidase-type tryparedoxin peroxidase of Trypanosoma brucei. *Biochem J* 405: 445–454, 2007.
42. Sztajer H, Gamain B, Aumann KD, Slomianny C, Becker K, Brigelius-Flohé R, and Flohé L. The putative glutathione peroxidase gene of Plasmodium falciparum codes for a thioredoxin peroxidase. *J Biol Chem* 276: 7397–7403, 2001.
43. Takahashi K, Avissar N, Whitin J, and Cohen H. Purification and characterization of human plasma glutathione peroxidase: a selenoglycoprotein distinct from the known cellular enzyme. *Arch Biochem Biophys* 256: 677–686, 1987.
44. Toppo S, Vanin S, Bosello V, and Tosatto SCE. Evolutionary and structural insights into the multifacet glutathione peroxidase (GPx) superfamily. *Antioxid Redox Signal* This Issue.
45. Tosatto SC. The Victor/FRST function for model quality estimation. *J Comput Biol* 12: 1316–1327, 2005.
46. Tosatto SC, Bindewald E, Hesser J, and Manner R. A divide and conquer approach to fast loop modeling. *Protein Eng* 15: 279–286, 2002.
47. Tosatto SCE and Toppo S. Large-scale prediction of protein structure and function from sequence. *Curr Pharm Des* 12: 2067–2086, 2006.
48. Ursini F, Heim S, Kiess M, Maiorino M, Roveri A, Wissing J, and Flohé L. Dual function of the selenoprotein PHGPx during sperm maturation. *Science* 285: 1393–1396, 1999.

49. Ursini F, Maiorino M, Brigelius-Flohé R, Aumann KD, Roveri A, Schomburg D, and Flohé L. Diversity of glutathione peroxidases. *Methods Enzymol* 252: 38–53, 1995.
50. Ursini F, Maiorino M, and Gregolin C. The selenoenzyme phospholipid hydroperoxide glutathione peroxidase. *Biochim Biophys Acta* 839: 62–70, 1985.
51. Ursini F, Maiorino M, and Roveri A. Phospholipid hydroperoxide glutathione peroxidase (PHGPx): more than an antioxidant enzyme? *Biomed Environ Sci* 10: 327–332, 1997.
52. Van Der Spoel D, Lindahl E, Hess B, Groenhof G, Mark AE, and Berendsen HJ. GROMACS: fast, flexible, and free. *J Comput Chem* 26: 1701–1718, 2005.
53. Veal EA, Day AM, and Morgan BA. Hydrogen peroxide sensing and signaling. *Mol Cell* 26: 1–14, 2007.
54. Villette S, Kyle JA, Brown KM, Pickard K, Milne JS, Nicol F, Arthur JR, and Hesketh JE. A novel single nucleotide polymorphism in the 3′ untranslated region of human glutathione peroxidase 4 influences lipoxygenase metabolism. *Blood Cells Mol Dis* 29: 174–178, 2002.
55. Wang HP, Schafer FQ, Goswami PC, Oberley LW, and Buettner GR. Phospholipid hydroperoxide glutathione peroxidase induces a delay in G1 of the cell cycle. *Free Radic Res* 37: 621–630, 2003.
56. Wendel A, Pilz W, Ladenstein R, Sawatzki G, and Weser U. Substrate-induced redox change of selenium in glutathione peroxidase studied by x-ray photoelectron spectroscopy. *Biochim Biophys Acta* 377: 211–215, 1975.

Address reprint requests to:
Matilde Maiorino
Department of Biological Chemistry
Viale G. Colombo, 3
I-35121 Padova, Italy

E-mail: matilde.maiorino@unipd.it

Date of first submission to ARS Central, February 24, 2008; date of final revised submission, February 25, 2008; date of acceptance, March 6, 2008.

This article has been cited by:

1. Xin Wang, Xudong Xu. 2012. Molecular cloning and functional analyses of glutathione peroxidase homologous genes from Chlorella sp. NJ-18. *Gene* **501**:1, 17-23. [CrossRef]
2. Etsuo NikiLipid Peroxidation . [CrossRef]
3. Federico Fogolari, Alessandra Corazza, Stefano Toppo, Silvio C. E. Tosatto, Paolo Viglino, Fulvio Ursini, Gennaro Esposito. 2012. Studying Interactions by Molecular Dynamics Simulations at High Concentration. *Journal of Biomedicine and Biotechnology* **2012**, 1-9. [CrossRef]
4. Roberto I. López-Cruz, Alcir Luiz Dafre, Danilo Wilhelm FilhoOxidative Stress in Sharks and Rays 157-164. [CrossRef]
5. Edith Lubos , Joseph Loscalzo , Diane E. Handy . 2011. Glutathione Peroxidase-1 in Health and Disease: From Molecular Mechanisms to Therapeutic Opportunities. *Antioxidants & Redox Signaling* **15**:7, 1957-1997. [Abstract] [Full Text HTML] [Full Text PDF] [Full Text PDF with Links]
6. Leopold Flohé , Stefano Toppo , Giorgio Cozza , Fulvio Ursini . 2011. A Comparison of Thiol Peroxidase Mechanisms. *Antioxidants & Redox Signaling* **15**:3, 763-780. [Abstract] [Full Text HTML] [Full Text PDF] [Full Text PDF with Links]
7. A. J. M. Martin, M. Vidotto, F. Boscariol, T. Di Domenico, I. Walsh, S. C. E. Tosatto. 2011. RING: networking interacting residues, evolutionary information and energetics in protein structures. *Bioinformatics* **27**:14, 2003-2005. [CrossRef]
8. Goedele Roos, Joris Messens. 2011. Protein sulfenic acid formation: From cellular damage to redox regulation. *Free Radical Biology and Medicine* **51**:2, 314-326. [CrossRef]
9. Gerardo Ferrer-Sueta, Bruno Manta, Horacio Botti, Rafael Radi, Madia Trujillo, Ana Denicola. 2011. Factors Affecting Protein Thiol Reactivity and Specificity in Peroxide Reduction. *Chemical Research in Toxicology* **24**:4, 434-450. [CrossRef]
10. Christina L. Takanishi, Li-Hua Ma, Matthew J. Wood. 2010. The role of active site residues in the oxidant specificity of the Orp1 thiol peroxidase#. *Biochemical and Biophysical Research Communications* **403**:1, 46-51. [CrossRef]
11. José Rafael Pedrajas , C. Alicia Padilla , Brian McDonagh , José Antonio Bárcena . 2010. Glutaredoxin Participates in the Reduction of Peroxides by the Mitochondrial 1-CYS Peroxiredoxin in Saccharomyces cerevisiae. *Antioxidants & Redox Signaling* **13**:3, 249-258. [Abstract] [Full Text HTML] [Full Text PDF] [Full Text PDF with Links]
12. Claudia Muhle-Goll, Florian Füller, Anne S. Ulrich, R. Luise Krauth-Siegel. 2010. The conserved Cys76 plays a crucial role for the conformation of reduced glutathione peroxidase-type tryparedoxin peroxidase. *FEBS Letters* **584**:5, 1027-1032. [CrossRef]
13. Daniela Dimastrogiovanni, Massimiliano Anselmi, Adriana Erica Miele, Giovanna Boumis, Linn Petersson, Francesco Angelucci, Alfredo Di Nola, Maurizio Brunori, Andrea Bellelli. 2010. Combining crystallography and molecular dynamics: The case of Schistosoma mansoni phospholipid glutathione peroxidase. *Proteins: Structure, Function, and Bioinformatics* **78**:2, 259-270. [CrossRef]
14. Shreenal Patel, Syeed Hussain, Richard Harris, Sunita Sardiwal, John M. Kelly, Shane R. Wilkinson, Paul C. Driscoll, Snezana Djordjevic. 2010. Structural insights into the catalytic mechanism of Trypanosoma cruzi GPXI (glutathione peroxidase-like enzyme I). *Biochemical Journal* **425**:3, 513-522. [CrossRef]
15. Stefano Toppo, Leopold Flohé, Fulvio Ursini, Stefano Vanin, Matilde Maiorino. 2009. Catalytic mechanisms and specificities of glutathione peroxidases: Variations of a basic scheme. *Biochimica et Biophysica Acta (BBA) - General Subjects* **1790**:11, 1486-1500. [CrossRef]
16. Edit Hermesz, Ágnes Ferencz. 2009. Identification of two phospholipid hydroperoxide glutathione peroxidase (gpx4) genes in common carp. *Comparative Biochemistry and Physiology Part C: Toxicology & Pharmacology* **150**:1, 101-106. [CrossRef]
17. Leopold Flohé , Fulvio Ursini . 2008. Peroxidase: A Term of Many Meanings. *Antioxidants & Redox Signaling* **10**:9, 1485-1490. [Abstract] [Full Text PDF] [Full Text PDF with Links]